Different influences of organic ligands on vivianite formation and dissolution

Banke, Sophie; Cottineau, Julien; Prot, Thomas; Korving, Leon; van Loosdrecht, Mark C.M.

DOI
10.1016/j.jece.2024.115139

Publication date
2025

Document Version
Final published version

Published in
Journal of Environmental Chemical Engineering

Journal of Environmental Chemical Engineering 13 (2025) 115139

Contents lists available at ScienceDirect

Journal of Environmental Chemical Engineering

journal homepage: www.elsevier.com/locate/jece

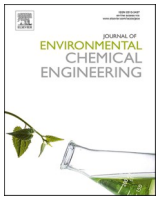

Different influences of organic ligands on vivianite formation and dissolution

Sophie Banke [a,b,*], Julien Cottineau [a], Thomas Prot [a], Leon Korving [a], Mark C.M. van Loosdrecht [b]

[a] Wetsus, European Centre of Excellence for Sustainable Water Technology, Oostergoweg 7, Leeuwarden 8911 MA, the Netherlands
[b] Biotechnology Department, Faculty of Applied Sciences, Delft University of Technology, Van der Maasweg 9, Delft 2629 Hz, the Netherlands

ARTICLE INFO

Keywords:
Iron complexation
Manure organic matter
Organic ligands
Phosphorus recovery
Vivianite

ABSTRACT

Vivianite ($Fe_3(PO_4)_2{\cdot}8\ H_2O$) has emerged as a promising mineral for phosphorus (P) recovery from digested sludge, and it may also contribute to phosphate management in lake sediments and manure, given the similar anaerobic conditions across these environments. However, organic ligands in these matrices have been proposed to complex with iron (Fe), thereby reducing the efficiency of vivianite formation. This study aims to elucidate the impact of organic ligands on vivianite formation, particularly focusing on their binding strength with iron and the subsequent effects on vivianite formation in pig manure. Organic ligands not only form complexes with iron but also influence the crystal growth process. We investigated how different organic ligands affect the formation and dissolution of vivianite, assuming that ligands with higher iron-binding strength would enhance phosphate solubilization. Our findings revealed that citrate nearly completely inhibited vivianite formation (up to 100 %) and caused a 50 % dissolution of existing vivianite, while humate hindered vivianite formation by 40 % but only led to a 10 % dissolution. Interestingly, pig-derived dissolved organic matter had minimal effects on the precipitation of iron and phosphorus but significantly altered the morphology of the resulting products, which varied depending on the age of the manure filtrate. While the iron binding strength of organic ligands does influence vivianite formation, it does not solely account for the reduced vivianite formation observed in complex matrices like manure. Therefore, a more nuanced assessment of the role of organic matter in vivianite formation is warranted.

1. Introduction

Vivianite ($Fe_3(PO_4)_2{\cdot}8\ H_2O$) is a key mineral in phosphorus recovery from wastewater, binding up to 70–90 % of the phosphorus present in anaerobic digesters [1]. Phosphate recovery as vivianite is advantageous due to its formation within a moderate pH range of 6–8 [2], its low solubility [3], its applicability as an iron fertilizer [4], and its potential use as a precursor for $LiFePO_4$ batteries [5]. Additionally, its paramagnetic properties enable a straightforward magnetic-based recovery process. Pilot-scale recovery of vivianite from digested municipal wastewater sludge has already been demonstrated [6]. While vivianite naturally occurs in lake sediments, its formation in these environments is less predictable than in digested sludge [7]. Manure may offer an alternative matrix for vivianite-mediated phosphate recovery, facilitating land application of the manure after phosphate removal in areas of high livestock production. The anaerobic conditions in manure should be conducive to vivianite formation, though prior research indicates that competing components in manure can interfere with iron availability [8].

Iron-organic interactions are central to various environmental processes. For instance, organic matter affects the weathering and reformation of iron oxides in soils, enhancing iron availability [9]. It also mobilizes iron (II) during river bank filtration [10], while small organic acids, such as citric and oxalic acids, dissolve iron oxides and release adsorbed phosphorus [11]. Lalonde et al. [12] reported that up to 20 % of organic carbon in sediments is associated with iron phases. Building on this, Kleeberg et al. [13] estimated that approximately 25 % of organic carbon in lake sediments binds to iron, thereby limiting the formation of vivianite.

Organic ligands have been hypothesized to impact vivianite

* Corresponding author at: Wetsus, European Centre of Excellence for Sustainable Water Technology, Oostergoweg 7, Leeuwarden 8911 MA, the Netherlands
E-mail addresses: sophie.banke@wetsus.nl (S. Banke), julien.cottineau@wetsus.nl, julien.cottineau@uha.fr (J. Cottineau), thomas.prot@wetsus.nl (T. Prot), leon.korving@wetsus.nl (L. Korving), M.C.M.vanLoosdrecht@tudelft.nl (M.C.M. van Loosdrecht).

https://doi.org/10.1016/j.jece.2024.115139
Received 28 June 2024; Received in revised form 9 December 2024; Accepted 15 December 2024
Available online 16 December 2024

formation [14,15]. Alginate and humate have been shown to limit vivianite formation at a concentration of around 1 g/L [16–19]. At high levels (10 g/L) acetate can also inhibit vivianite formation, though effects are minimal at concentrations below 5 g/L [18]. Vivianite dissolution by organic ligands has also been previously studied. For example, Yang et al. [20] and Gypser and Freese [21] observed that citrate partially dissolves vivianite at pH 6, while the effect of humate on vivianite dissolution was minimal under similar conditions [21]. Despite these findings, a systematic framework to correlate organic ligand concentrations with vivianite formation efficiency is lacking, and the influence of iron-binding strength has yet to be directly investigated.

During vivianite formation, organic ligands with high iron-binding strength should make iron unavailable for vivianite formation. However, inhibition could also arise if organic ligands bind to vivianite crystal nuclei, impeding further crystal growth [16,22]. Nevertheless, iron-organic binding strength should be the primary factor driving vivianite dissolution forward until the thermodynamic equilibrium is reached. Hence, the extent of vivianite dissolution by an organic ligand should give insight into the degree of the iron-binding strength.

Previous studies have largely focused on the effects of organic ligands on either vivianite formation [16–19,22,23] or vivianite dissolution [20,21,24]. By addressing both formation and dissolution, which was not realized in previous research, we aim to elucidate how iron-complexing organic ligands influence vivianite formation and evaluate the role they could play in manure. Given the complexity of manure, we opted for a comparative approach, examining dissolved organic matter in manure alongside those in controlled systems relevant to vivianite formation. Our approach offers a novel perspective on the complex interactions between organic ligands and vivianite formation, with potentially surprising insights for phosphate recovery in manure systems.

2. Materials and methods

2.1. Organic ligands

This study examines the effects of several organic compounds on vivianite formation and dissolution, selecting organics that are chemically relevant to vivianite:

- **Bipyridine** has been proposed as a potential extractant for quantifying vivianite due to its specific affinity for iron (II) bound within vivianite [25,26].
- **Citrate**, a small molecule exuded by plant roots, is frequently used to evaluate the bioavailability of phosphorus fertilizers [27].
- **Volatile fatty acids** are key transformation products arising during the anaerobic digestion of organic materials such as sludge and manure [28,29]. Acetate serves as a representative compound of this group.
- **Humate**, a stable degradation product of organic matter, forms in complex matrices like sewage sludge, manure, and sediments. Its structure includes functional groups that can effectively complex metal ions, including Fe [30].
- **Alginate** represents polysaccharides, the most abundant natural biopolymers, and is relevant in the context of food science and waste management [31].
- **Pig dissolved organic matter (DOM)**, derived from pig manure filtrate, was included to represent a real environmental matrix and provide a comparison against the more defined organic compounds. Given the biological activity in manure, which drives continuous organic matter degradation, pig DOM solutions aged for three and six months were tested.

Proteins were excluded based on prior findings from Li et al. [19], who observed negligible effects on vivianite formation using Bovine Serum Albumin. Similarly, amino acids like alanine and aspartic acid have minimal impact on phosphate precipitation with iron (III) [32], and their iron (II) complex formation constants are even lower [33].

Preparation of pig DOM and humate solutions involved centrifugation (Beckman Coulter, Avanti J-15R) of raw pig manure at 25,000 rpm for 10 minutes to address the poor settling properties of pig manure. The humate solution was processed similarly to allow for better comparability with the manure filtrate. Supernatants from these preparations were then filtered through 0.45 μm filters and dissolved organic carbon (DOC) served as the baseline for comparing the different organics. Setting the DOC concentration to a uniform level ensured consistent comparability among organic ligands, based on literature from sediment studies that estimate iron binding relative to organic carbon [13]. For each ligand, a stock solution with a DOC concentration of 730 mg/L was prepared (see Table A4), followed by dilution to a target concentration of 330 mg/L. This concentration was selected because it is equivalent to a 1 g/L humate solution, a level used in the dissolution study by Gypser and Freese [21] and to balance solubility constraints, particularly for less soluble compounds like bipyridine and humate.

2.2. Dissolution and formation experiments

All experiments were carried out in triplicate in serum bottles in a glove box under a nitrogen atmosphere ($O_2 < 100$ ppm).

For the dissolution experiments, 50 mg of synthetic vivianite was mixed with 100 mL of organic solution. Vivianite for the dissolution experiment was synthesized at room temperature from solutions of 600 mM K_2HPO_4 (*VWR Chemicals BDH*) and 900 mM $FeCl_2{\cdot}4\ H_2O$ (Sigma Aldrich). Solutions (50 mL) were mixed under anaerobic conditions in a glove box, and the precipitated solid was then washed three times with ultrapure water and dried in the glove box in the dark.

For the formation experiments, a phosphate solution was prepared by adding 5 mL of 40 mM K_2HPO_4 stock solution to 45 mL of the organic solution, and an iron solution was prepared by adding 5 mL of a 60 mM $FeCl_2{\cdot}4\ H_2O$ stock solution to 45 mL ultrapure water. The iron and phosphate solutions were mixed together, aiming at a Fe/P ratio of 1.5 according to vivianite stoichiometry. The pH was measured by potentiometry and adjusted to pH 8 with 1 M NaOH or 1 M HCl for each sample. Negative controls were prepared for humate and pig DOM experiments containing only humate and pig DOM solutions. Formation and dissolution experiments were replicated without organics in ultrapure water.

The samples were agitated at 120 rpm at room temperature on a rotary platform shaker (*Heidolph, Unimax 2010*). Samples (1.5 mL for dissolution, and 1 mL for formation) were taken after 1 h, 4 h, 24 h, 48 h, and 168 h with subsequent filtering through 0.45 μm filters. At the end of the experiment, the pH was measured again. All samples were centrifuged (*Beckman Coulter, Avanti J-15R*) at 4750 rpm for 10 min to efficiently settle most of the solids that are formed when synthesizing vivianite in an aqueous matrix, washed twice with 50 mL of ultrapure water, and centrifuged at the same settings. The remaining solid particles were dried in the air at room temperature, and the yield was determined.

2.3. Analysis

Iron and phosphorus concentrations from vivianite formation and dissolution experiments were monitored with ICP-OES measurements (Perkin Elmer, Optima 5300 DV). The filtered samples were diluted and topped with 300 μl HNO_3 (69 %). The ICP-OES was equipped with an Autosampler, Perkin Elmer, type ESI-SC-4 DX fast, and the data were processed with the software Perkin Elmer WinLab32. The rinse and standard internal solutions were 2 %HNO_3 and 10 mg/L of Yttrium. The DOC (Shimadzu DOC-L) was measured for every ligand solution to normalize the results with the exact DOC in the samples.

Synthetic vivianite and solids were characterized by determining the Fe/P ratio by digestion in 69 % nitric acid with subsequent ICP-OES

analysis. Attenuated Total Reflectance Infrared ATR IR spectroscopy (Bruker Alpha II) was measured by tightly pressing 1–2 mg of solid on the crystal. The received spectra were converted to transmission, baseline corrected using the rubberband method (64 points) and normalized to the highest intensity. X-Ray Diffractometry (XRD) (Bruker D8 Advance diffractometer) was performed by depositing the powder on a Si510 wafer, measuring with Cu Ka radiation (Coupled θ −2θ scan 5° - 80°, step size 0.020 ° 2θ, counting time per step 2 s), and using Burker software DiffracSuite.EVA vs. 6 for data evaluation. SEM (Scanning Electron Microscopy) (JEOL JSM-6480LV) was prepared by coating the solids with a 10 nm layer of gold at 15 Pa and 25 mA to make the surface electrically conductive. SEM was executed at 6 kV accelerating voltage, 10 mm working distance, and using JEOL SEM Control User Interface.

3. Results

3.1. Solution chemistry

3.1.1. Phosphate dissolved from vivianite in the presence of organic ligands

In the initial phase of this study, the evolution of phosphate concentrations in solution was monitored to assess vivianite dissolution in the presence of each organic ligand (Fig. 1). The ligands could be grouped into three categories based on their effects:

- Bipyridine and citrate exhibited the most pronounced vivianite dissolution capacity. After one week, bipyridine and citrate dissolved 39 % and 31 % of the vivianite, respectively, based on solubilized phosphorus. Notably, equilibrium for citrate had not been achieved even after one week, indicating continued dissolution potential (Figure A2).
- Humate and three-month-old pig DOM induced moderate vivianite dissolution, with phosphorus release reaching up to 6 % by the end of the experiment. Though both humate and 3-month-old pig DOM contributed to vivianite dissolution, their effects were minor compared to those of bipyridine and citrate.
- Acetate, alginate, 6-month-old pig DOM, and ultrapure water showed minimal impact on vivianite dissolution, with solubilized phosphorus concentrations remaining below 3 % after 16 h. These ligands displayed negligible dissolution capabilities relative to the significant effects observed with bipyridine and citrate.

3.1.2. Phosphate left in the solution during vivianite formation in the presence of organic ligands

To assess the relationship between vivianite dissolution capacity and inhibition of vivianite formation by organic ligands, the phosphorus concentration in solution during vivianite formation was analyzed for each substance (Fig. 2).

In the control with ultrapure water, where no organic ligands were

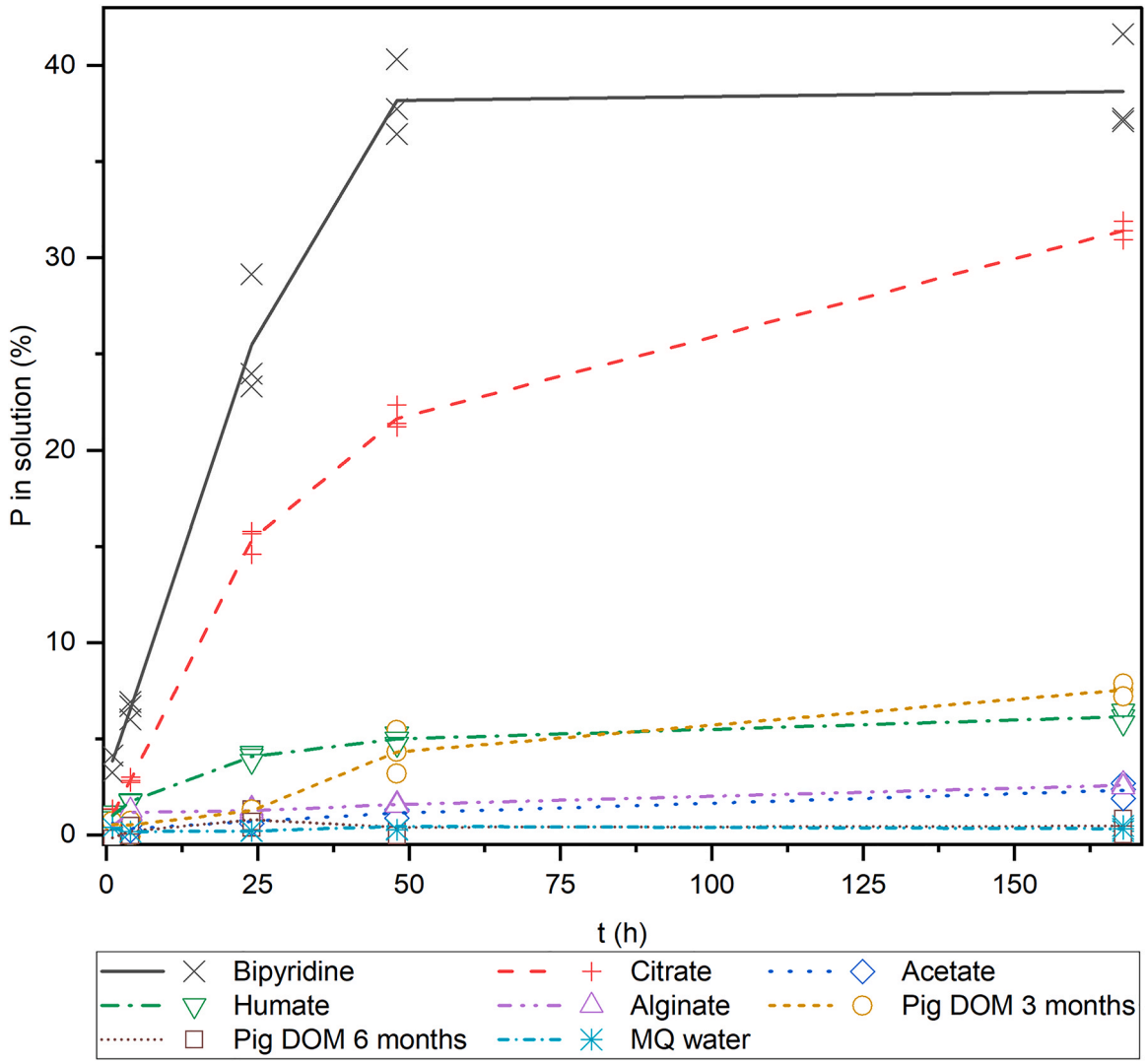

Fig. 1. Phosphate dissolution from vivianite after addition of organic ligands (DOC 330 mg/L). Start concentration of vivianite was 60 mgP/L.

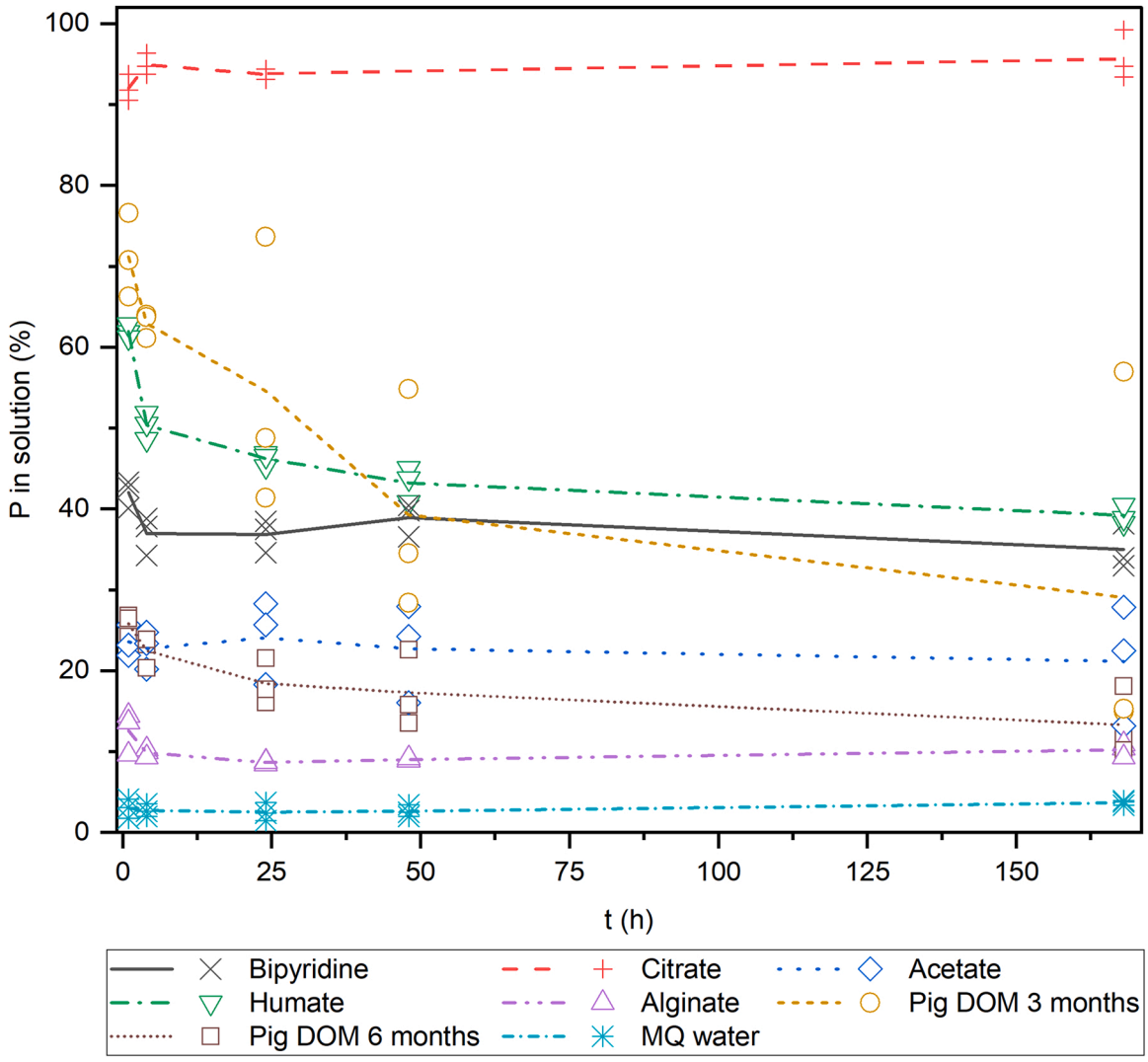

Fig. 2. Influence of organic matter on vivianite formation, phosphate remaining in solution after start of crystallization experiment. Organic compounds were dosed at a DOC of 330 mg/L. Start concentration for phosphate was 60 mgP/L.

present, nearly all phosphorus precipitated within the first hour, leaving about 4 % in solution. In contrast, solutions containing organic ligands took longer to reach equilibrium, typically stabilizing after approximately 4 h. However, in both pig DOM solutions, phosphorus concentration continued to decrease significantly even beyond 48 h. For humate, a slight decrease in phosphorus concentration was observed after 4 h, with a gradual decline continuing up to 168 h.

Among the organic ligands, citrate displayed the strongest inhibitory effect on vivianite formation, retaining 96 % of phosphorus in solution. Humate and bipyridine also substantially inhibited phosphorus precipitation, with 39 % and 35 % remaining in solution, respectively. In comparison, alginate, acetate, and the two pig DOM solutions demonstrated a milder inhibitory effect on phosphorus precipitation, with 10–20 % of phosphorus retained in the solution.

3.2. Solid phase analysis

Precipitates were collected by centrifugation (Figure A 3) and subsequently analyzed using XRD, IR spectroscopy, and SEM patterns (Fig. 3). XRD indicated the presence of vivianite in all recovered solids except for the precipitate from the 6-month-old pig DOM solution. This precipitate exhibited a high degree of amorphousness, as indicated by a broad hump centered around 20° 2θ, which prevented clear identification by XRD.

The IR spectra of all recovered precipitates, except for the 6-month pig DOM sample, displayed features consistent with the vivianite reference spectrum. Characteristic vivianite bands (Fig. 4, Table A3) include the hydroxyl stretching around 3200 cm^{-1}, HOH bending around 1600 cm^{-1}, P-O stretching bands near 1000 cm^{-1}, water liberational vibrations around 800 cm^{-1}, and out-of-plane bends near 500 cm^{-1} [36]. Additional bands around 1440 cm^{-1} (highlighted in red in Fig. 4) were noted in the spectra for humate and pig DOM precipitates. These bands correspond to organic carbon-related bonds, such as C-H scissoring, C═C breathing, and phenolic C-O stretching [37].

The SEM images of precipitates formed from different ligand solutions are presented in Fig. 5 at 5000× magnification to show the crystal structure and 2000× magnification in Figure A6 to show precipitated flocks. In ultrapure water, vivianite predominantly forms small plate-like structures that assemble into flower-like clusters approximately 5 μm in diameter. When precipitated in bipyridine solution, two phases appear: one of small, rounded, porous aggregates, and another comprising elongated plates about 10 μm in length. Vivianite formed in an acetate solution shows a structure of larger, pointed, fan-shaped plates (over 10 μm) stacked in layers, with a secondary phase of small, rounded, porous formations interspersed.

In contrast, vivianite precipitated in humate, alginate, and 3-month-

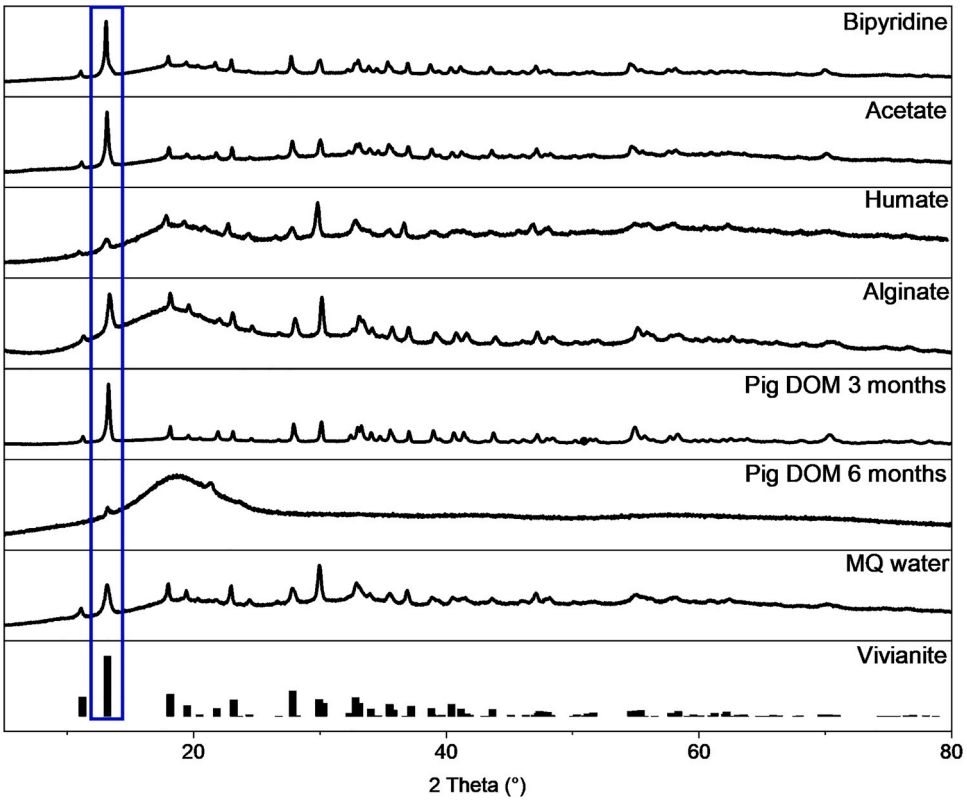

Fig. 3. XRD patterns of vivianite formed in the solutions with different organic ligands, including a reference synthetic vivianite [34] (bottom). The blue box indicates the main reflex for vivianite.

old pig DOM is composed of more isolated plates with rounded edges. For vivianite in alginate, small flower-like structures (1–2 μm) are observed, while the precipitate from humate shows accumulated, thicker plates less than 1 μm long. Plates formed in 3-month-old pig DOM are thin, roughly 10 μm in length, and occasionally assemble into flower-like formations. Meanwhile, vivianite precipitated in 6-month-old pig DOM yields a mix of thin, 2 μm long, vivianite-like plates (marked in red) and bigger flat plates (marked in green). Notably, only minimal precipitate was recovered from 6-month pig DOM samples following centrifugation, as shown in Figure A 3.

4. Discussion

4.1. Comparison of vivianite dissolution and formation potential of organics based on DOC

4.1.1. Comparison of the ligand strengths

To evaluate the effectiveness of organic ligands in dissolving vivianite and inhibiting its formation, the molar phosphate concentration in solution was normalized against the molar DOC concentration (Table A 1). The amount of phosphate remaining in or released to the solution was used as an indicator for the extent of vivianite formation or dissolution. Phosphate was chosen as a proxy for vivianite processes because, in typical scenarios, all phosphate is associated with vivianite when not in solution, whereas iron can precipitate as something other than vivianite. This is supported by the higher phosphorus-to-iron ratios observed in solution (Figure A 1) and the elevated Fe/P ratios in the recovered solids (Table A 3).

Fig. 6 presents the normalized data, with vivianite dissolution shown on the left side of the x-axis and vivianite formation on the right. The organic ligands are arranged from strongest to weakest dissolution potential in descending order (indicated by a thin red line). This order is mirrored on the formation side of the graph, marked by a thick red line. If data points on the formation side fall to the right of the thick red line, this suggests that the ligand has a greater inhibitory effect on vivianite formation than its dissolution potential alone would predict.

4.1.2. The role of iron-binding strength

Vivianite dissolution in the presence of organic ligands is likely driven by the complexation of free iron in solution [11,21,24]. Given the low solubility of vivianite ($K_{sp} = 10^{-35.76}$ [3] (Eq. 1)), the activity of dissolved iron and phosphate ions remains minimal at neutral pH:

$$K_{sp} = \left[Fe^{2+}\right]_{eq}^{3} \bullet \left[PO_4^{3-}\right]_{eq}^{2} \quad (1)$$

With $\left[Fe^{2+}\right]_{eq}$ and $\left[PO_4^{3-}\right]_{eq}$ the activity of iron and phosphate at equilibrium.

The addition of ligands induces vivianite dissolution by binding free iron in solution, thereby shifting the equilibrium toward further dissolution. The efficiency of a ligand in dissolving vivianite is generally related to its iron-binding strength, expressed by the complex formation constant

$$K_f = \frac{[Fe^{2+}{}_xOL_y]}{[Fe^{2+}]^x \bullet [OL]^y} \quad (2)$$

With $[Fe^{2+}]$ the iron concentration, $[OL]$ the concentration of the organic ligand and $[Fe^{2+}{}_xOL_y]$ the concentration of the iron-organic complex.

The ligand binding strength depends on the density and type of functional groups present [22]. Bipyridine, for instance, has a high affinity for iron (II) attributed to interactions between iron and the free electron pairs of the nitrogen [38]. Despite the high complex formation constant of bipyridine ($\log K_f = 17.5$ [39]), only 31 % of iron could theoretically be complexed due to stoichiometric limitations, as each iron ion requires three bipyridine molecules for binding. However, bipyridine dissolved 38.5 % of vivianite, possibly due to partially

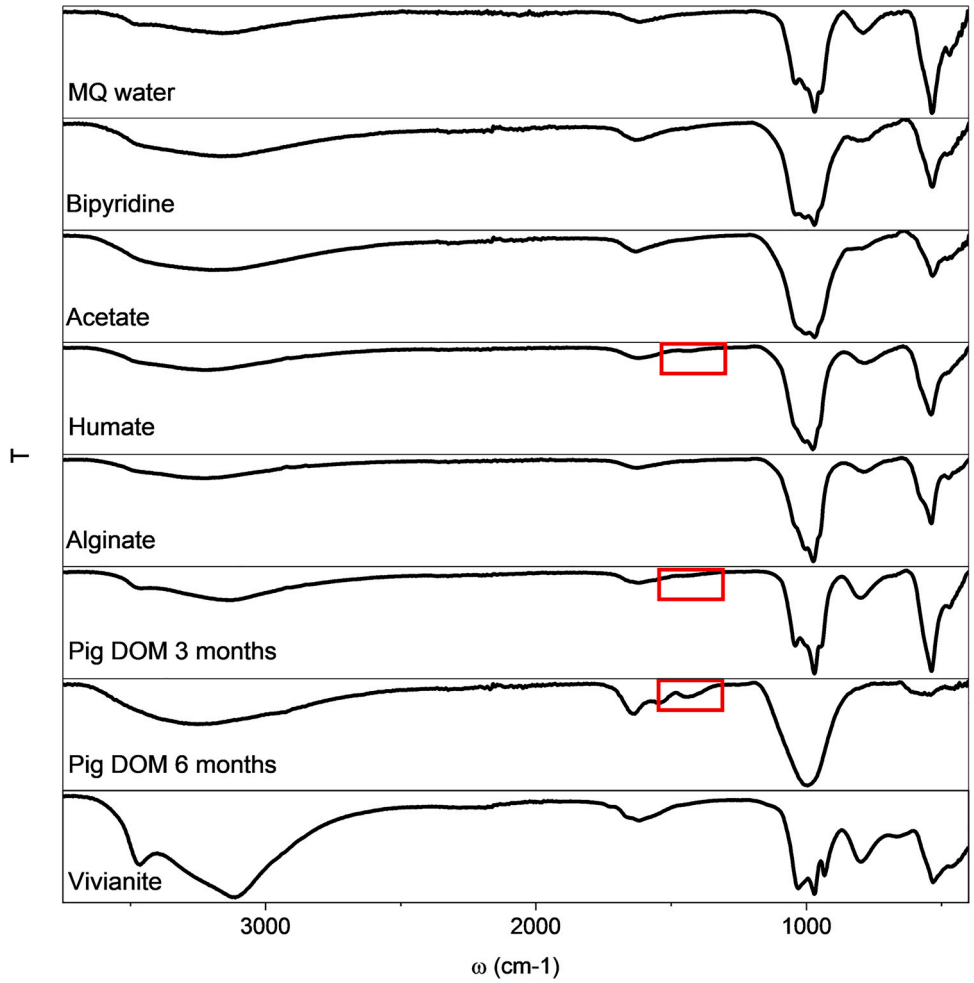

Fig. 4. IR spectra of precipitates formed in ligand solutions after washing with ultrapure water with reference vivianite from the Rruff database [35]. Bands marked in red could stem from organic residue (Table A 3).

binding with fewer than three molecules.

Other ligands primarily bind iron through deprotonated carboxylic (COO^-) and hydroxy (O^-) groups. Citrate, with three carboxylic and one hydroxy group, has a strong affinity for iron, with a $\log K_f = 5.89$ for the $[Fe\text{-citrate}]^-$ complex [40]. Although citrate could theoretically complex all available iron, it dissolved only 31 % of vivianite within the first week, suggesting equilibrium had not been reached (Figure A 2). Extended data indicates ongoing phosphorus release, aligning with findings by Gypser and Freese [21], who reported 80 % phosphate release from vivianite over 8 weeks.

The iron-binding strength of acetate is low, with $\log K_f = 1.4$ for the $[Fe\text{-acetate}]^+$ complex [40], which explains its low potential to dissolve vivianite. Interestingly, some humate-metal interactions have been described to resemble acetate-type binding [41]. Nonetheless, humate dissolved more vivianite than acetate. However, humate is not only able to interact with iron through carboxylic groups but also via phenolate ($ph\text{-}O^-$) and possibly sulfur or nitrogen-containing groups [30]. Yamamoto et al. [42] reported a $\log K_f = 5.8$ for iron-humate complexes at pH 5, which appears high since the iron citrate complex has a formation constant at a similar value, but citrate is dissolving significantly more vivianite. Gypser and Freese [21] similarly observed an 8 % vivianite dissolution with humate at pH 6 and DOC of 546 mg/L, comparable to the 6 % dissolution observed here. However, quantifying humate binding remains challenging due to its non-stoichiometric nature and dependence on origin.

In manure, iron is likely complexed by a mixture of polysaccharides, humate-like substances, and volatile fatty acids, with humate being the most potent among them. The capacity of 3-month-old pig DOM to dissolve vivianite likely reflects a humate-like composition of functional groups, while 6-month DOM, resembling alginate and acetate, showed minimal dissolution (Fig. 1). The increased humate-like behavior in fresher manure is unexpected, as aging generally favors humate precursors and depletes biodegradable polysaccharides [43]. Further analysis of organic transformations during manure aging could clarify these shifts in functionality.

In summary, small ligands like citrate and bipyridine show high iron binding strength and effectively dissolve vivianite. While natural organic matter, such as humate, also binds iron, its binding strength is insufficient for significant vivianite dissolution via complexation. Similarly, manure-derived DOM exhibited limited complexing ability. These dissolution experiments suggest that organic ligands can induce vivianite dissolution and influence its formation; however, binding strength alone does not fully explain their impact on vivianite formation, as further discussed in the following section.

4.1.3. *Vivianite formation vs dissolution*

For the organic ligands tested, aside from bipyridine, inhibition of vivianite formation appears more pronounced than their impact on vivianite dissolution. Previous studies have examined the role of ligands such as acetate, humate, and alginate in vivianite formation. When comparing findings, however, it is essential to consider not only the concentration of these organic ligands but also variables including initial phosphate concentration, Fe/P ratio, and pH (Table 1).

The impact of acetate on vivianite has been shown to be minor [18],

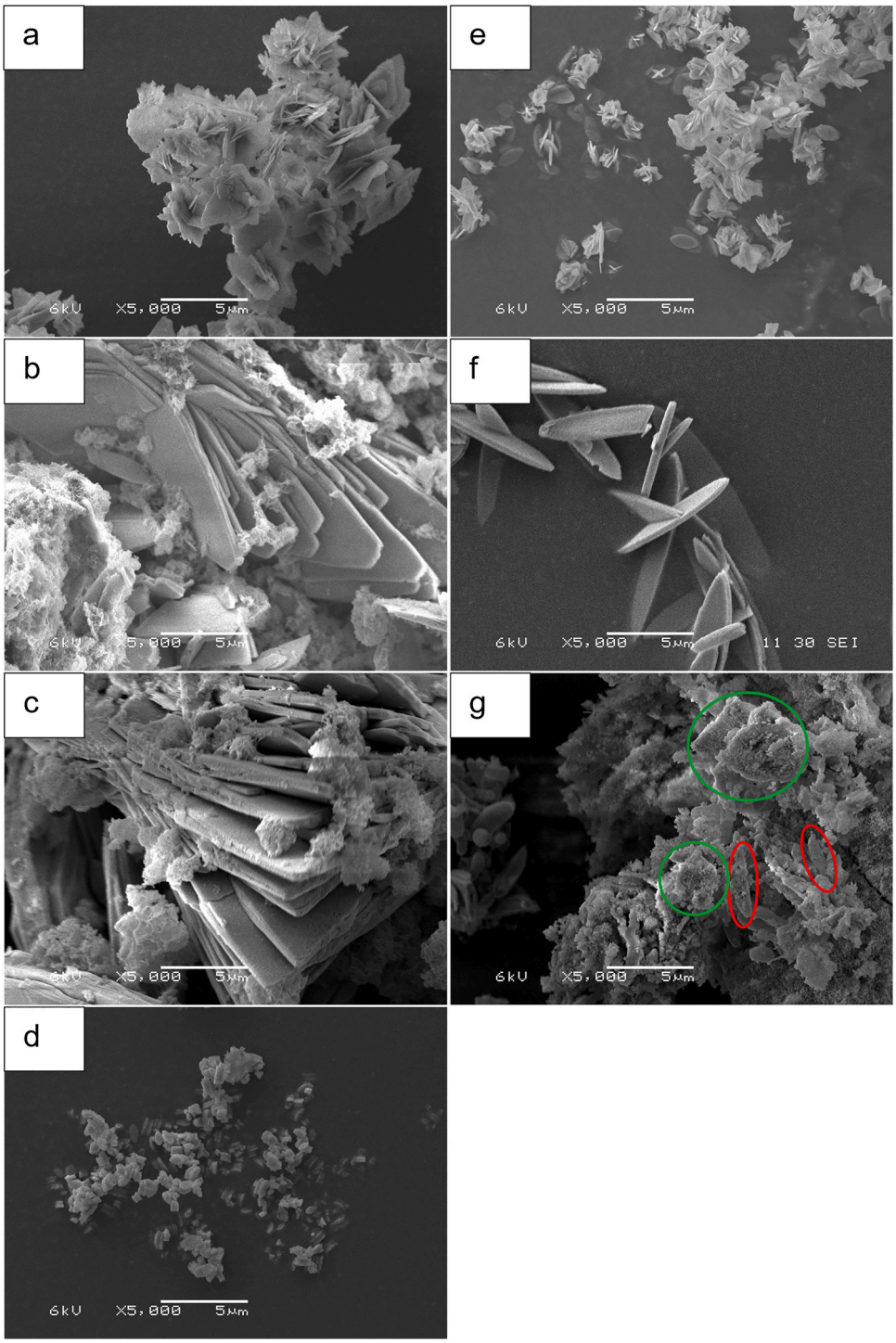

Fig. 5. SEM images of precipitates formed in different organic solutions at 5000x magnification with (a) MQ water, (b) bipyridine, (c) acetate, (d) humate, (e) alginate, (f) pig DOM 3 months, (g) pig DOM 6 months.

which aligns with its relatively weak iron-binding strength. In this study, however, the influence of acetate on vivianite formation was more pronounced, likely due to pH-induced iron oxidation effects. Under slightly alkaline conditions, iron(II) hydroxide precipitation is favored, and this phase readily oxidizes to iron(III) oxide [18,44]. Chen et al. also noted that acetate itself can enhance iron oxidation [18]. Iron oxide precipitates can still act as phosphate sinks through adsorption, which could have led to additional phosphate removal at pH 8 in this study in comparison to the results by Chen et al. at pH 6.

Similarly, humate displays a more substantial effect on vivianite formation than its iron-binding strength alone would suggest. In general, the inhibition of vivianite formation by humate intensifies with higher humate concentrations and lower phosphate levels (Table 1). In this study, 1 g/L humate and 2 mM phosphate concentrations were approximately half those used by Cui et al. [17] with 2.5 g/L humate and 4 mM phosphate. Yet, there seems to be a trend of around 40 % inhibition in vivianite formation at 1 mmol phosphate per 0.5 g humate.

Alginate impeded vivianite formation by 10 % in this study which was slightly greater than would be expected based on its iron-binding strength. Zhang et al. [16] reported comparably low inhibition levels

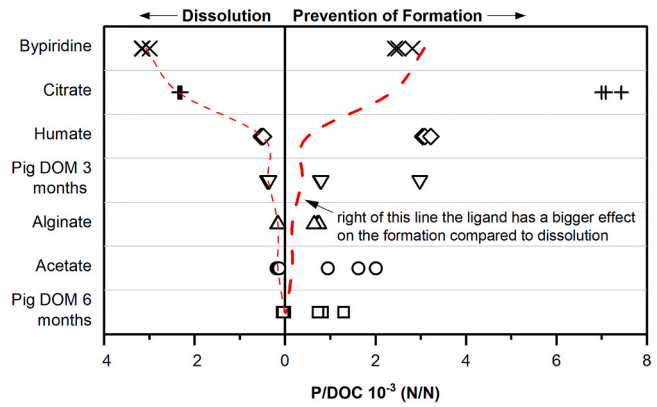

Fig. 6. Comparison of the vivianite dissolution and vivianite formation inhibition capacity for 7 organic ligands. P in solution per DOC (N/N) of each organic solution after 168 h (Table A 1). Left part of the axis: Organics organized by their Vivianite dissolution strength. Right part of the axis: Respective Vivianite formation prevention strength with trendline pointing out Vivianite dissolution strength.

Table 1
Vivianite formation inhibition of acetate, humate and alginate in this study and literature with starting phosphate concentration, organic ligand (OL) concentration, Fe/P ratio and pH.

	inhibition %	P (mM)	OL (g/L)	Fe/P	pH	study
acetate	5	4	4.72	1.5	6	[18]
	10		9.44			
	25	2	0.82	1.5	8	this study
humate	4	10	0.1	1.5	7	[19]
	30	4	2.5	1.5	6	[18]
	70		3.5			
	30	5	1.8	1.5	6.5	[17]
	60		2.5	2		
	40	2	1	1.5	8	this study
alginate	12	10	0.8	1.5	7	[19]
	30	5	0.88	1.5	6.5	[17]
	25		1.77	2		
	12	10	0.8	1.8	8	[16]
	10	2	1.13	1.5	8	this study

with 12 % inhibition at 0.8 g/L alginate, whereas Cui et al. [17] observed stronger inhibitory effects (30 %) at 0.88 g/L. Cui et al. performed their experiments at a pH of 6.5, which might have increased the effect of alginate in their case. Nevertheless, the role of alginate in vivianite inhibition appears to be less critical than the one of humate [17].

Pig DOM also shows stronger vivianite formation inhibition than would be expected based on iron-binding strength. Vivianite formation in three-month-old pig DOM shows a response similar to humate, whereas formation in six-month-old pig DOM more closely resembles that with alginate. This indicates that the composition and aging of pig DOM may dynamically influence vivianite crystallization, potentially reflecting shifts in its organic profile with age.

In the next step, factors beyond iron-binding strength that impact vivianite formation are evaluated:

- Iron-organic complexation occurs more rapidly than vivianite formation

  Since vivianite formation is notably more efficient than vivianite formation, the process is unlikely to be thermodynamically driven. If iron-organic complexes form more quickly than vivianite during its formation phase, this could lead to a supersaturation level insufficient for vivianite nucleation, thereby limiting its precipitation. Wei et al. observed that humate can reduce supersaturation through Mg^{2+} complexation in struvite crystallization [45]. Iron-organic complexation may offer a kinetic advantage over vivianite formation, as only one type of binding—between the functional group and iron—is necessary. In contrast, vivianite formation requires a more organized structure, with specific binding environments at two iron sites. Statistically, this organized arrangement is less probable than iron binding to the functional group of an organic ligand. Thus, this kinetic advantage alone could account for the discrepancy between the efficiencies of vivianite dissolution and formation.
- Organic ligands binding to vivianite crystal nuclei

  Li et al. [22] proposed that iron-humate binding might extend the Fe-O-P bond length within vivianite clusters. Coordination of an organic ligand to these clusters may destabilize them, thereby lowering the nucleation rate and size of vivianite crystals. Compared to precipitation in ultrapure water, vivianite formation in the presence of organic ligands was observed to be slower, supporting the hypothesis that organic-ligand interactions with crystal nuclei can impede nucleation. This reduction in nucleation rate due to organic binding to crystal nuclei could play a role in inhibiting vivianite formation.
- Organics blocking crystal growth sites

  Wei et al. [46] noted that humate blocked growth sites on struvite crystals, and Zhang et al. [16] suggested a similar role for alginate in vivianite inhibition. Since pig DOM contains polysaccharides, humate precursors, and various organic macromolecules, it is plausible that similar site-blocking effects could contribute to vivianite inhibition in this matrix. Such organic macromolecules may obstruct crystal growth sites, further hindering vivianite formation.

4.1.4. Evaluation of DOC as a base of comparison

In this study, the iron binding affinities of various organic compounds were investigated by examining the influence of dissolved organic carbon concentration on vivianite formation and dissolution. Using DOC as a normalization approach offers a practical advantage: since any organic substance in natural environments contains carbon, DOC analysis provides a feasible method for estimating iron binding across diverse systems. This approach aligns with the hypothesis proposed by Kleeberg et al. [13], which suggests that around 25 % of organic carbon in natural environments is bound to iron. However, our findings demonstrate variability in iron binding across different organic types. For instance, alginate limited vivianite formation by binding approximately 10 % of iron, while pig DOM bound 10–20 %, and humate displayed a higher binding potential, sequestering 40 % of iron. These findings suggest that while Kleeberg's 25 % assumption provides a rough approximation, individual organic compounds like humate may exhibit considerably higher iron binding capacities. This implies that sediment iron binding potential could be better predicted by assessing humate content specifically, rather than assuming a uniform 25 % binding capacity.

One limitation of normalization by DOC is its inability to account for the specific functional groups that influence iron binding strength, as binding affinities depend on more than just carbon content. While alternative quantification techniques could target these specific interactions, many were not feasible for this study. For example, pH titration can identify charged functional groups [45] but would overlook non-charged groups like nitrogen in bipyridine. Another approach, following the iron titration method of Gould and Genetelli [47], could capture all iron-binding components within each organic compound mixture, allowing a comprehensive comparison across organic solutions. Adjusting this method for systems containing iron, phosphate, and organics could, therefore, offer a more nuanced understanding of organic interactions with vivianite.

Ideally, the iron binding should be assessed in terms of stoichiometry; however, quantifying binding capacity in molar terms is challenging for some organics. While straightforward for small, defined compounds like bipyridine and citrate, it is less feasible for polymeric or complex mixtures like alginate, humate, and pig DOM. The latter

contains macromolecules with variable structures, alongside biopolymers and smaller ligands, complicating efforts to standardize binding comparisons across organic types.

4.2. Precipitates vary in the presence of different organic ligands

The precipitates formed exhibit different characteristics, such as morphology and settleability after centrifugation (Fig. 5, Figure A 3).

The crystal size of vivianite synthesized in acetate and bipyridine solutions appears to be larger than that of the vivianite formed in MQ water or in the presence of other organic ligands. This observation may be attributed to a reduction in supersaturation index (SI) caused by decreased soluble iron levels. Moreover, the secondary phase could be due to iron(III) oxide formation [18] as explained in Section 4.1.2.

The morphology of vivianite precipitates varies when humate is present. For instance, Li et al. [19] documented flower-like structures with thin plates like those observed in MQ water, while Cui et al. [17] identified irregular shapes, and Chen et al. [18] observed compact, thick plates similar to those in this study. Considering humate iron binding seemed to depend on the type of humate, morphology may also be linked to humate type. Further, the concentration ratio of humate to phosphate appears critical, as demonstrated by Cui et al. [17].

At alginate concentrations above 400 mg/L with an initial phosphate concentration of 10 mM, Zhang et al. [16] observed morphological shifts in vivianite. In the present study, however, alginate concentrations were approximately 1 g/L, with phosphate concentrations of 2 mM. Under these conditions, vivianite morphology largely resembled that in MQ water, albeit with smaller crystals. Organic adsorption on crystal surfaces could have contributed to smaller particle size and worse settling properties [16] (Figure A 3).

The elongated plate morphology of vivianite precipitated in three-month-aged pig DOM is similar to that observed in vivianite formed with manganese and magnesium under high salinity conditions [48]. While ICP analysis did not detect elevated magnesium in the precipitates, high salinity levels in pig DOM were evident. Organic adsorption onto the crystals may further influence morphological characteristics.

In contrast, vivianite formed in six-month-old pig DOM was less crystalline, as evidenced by the lack of clear XRD peaks, though a reflex within the characteristic vivianite region (14° 2θ) was present. SEM imaging revealed mixed phases, with some elongated plates resembling those in three-month pig DOM (circled in red), suggesting limited vivianite formation. The other precipitates observed could stem from organic matter as indicated by IR measurements and iron oxide formation. Elevated pH and volatile fatty acids, similar to the acetate solution conditions, could have contributed to iron oxide precipitation. One reason for decreased vivianite formation in 6-month-old pig DOM could be the prolonged induction time for vivianite crystallization, as proposed by Schott et al. [49] to explain the poor crystallinity of calcium phosphate in pig manure. During pig manure aging, compounds that extend the induction phase of vivianite crystallization could be formed.

The following factors influence the characteristics of vivianite crystals:

- **Saturation Index:** For optimal crystal growth, the SI of the solution must fall within the narrow meta-stable zone of vivianite [50]. If the SI is excessively high, precipitation occurs quickly, producing smaller, less crystalline solids. Conversely, if SI is too low, precipitation is unlikely. Iron-complexing ligands can reduce SI, helping to reach the meta-stable zone and thereby promoting larger, well-formed crystals.
- **Organic Adsorption on Vivianite:** Organic compounds can attach to the growth sites of vivianite, affecting crystal shape and size, as discussed in Section 4.1.2. During crystal growth, flat plates are stacked, forming step-like structures. Organic adsorption at these steps alters the energy required for further growth, potentially favoring rounded rather than plate-like shapes [51]. Adsorption can also block growth sites, leading to smaller crystals [22]. Additionally, adsorbed organics alter the surface charge of crystals; if the surface charge increases, repulsive forces between particles also increase, resulting in poorer settleability [46].
- **Interfering Ions:** Pig DOM and humate solutions contain various ions, such as Mg, K, and Ca, which may interfere with vivianite crystallization. These ions can block growth sites on crystals or be incorporated in the structure itself [48].

4.3. Outlook

We investigated the influence of iron binding strength on vivianite formation due to challenges in promoting efficient vivianite crystallization in manure. Previous studies have attributed limited vivianite formation to organic interference across various environments, including lake sediments [13], digested sludge [19], hydrothermal sludge [23], and urine [14]. This prompted us to explore a similar hypothesis for manure. However, our results suggest that dissolved organic matter in manure does not complex iron as extensively as anticipated. This led us to conclude that organics are sometimes overly attributed with influencing vivianite formation, and that studying organic effects within a complex matrix like manure is significantly more challenging than in controlled, clean conditions.

Through this work, we also gained insights into the behavior of specific organic ligands. Citrate, for example, often serves as an indicator of bioavailability [27]. In our study, a sustained release of phosphorus from vivianite was observed in presence of citrate, which aligns with previous research by Yang et al. [20] suggesting the potential of vivianite as a slow-release fertilizer. This finding may particularly renew interest in vivianite as a source of iron fertilizer in agricultural applications.

In lake sediments, where more recalcitrant organic compounds like humates are prevalent, iron binding is likely dominated by humates. Sediments also typically contain lower phosphate levels compared to digested sludge. Higher humate levels and lower phosphate levels could reduce vivianite formation since iron would be more likely to be bound by humate. Testing this hypothesis through a focused study on the composition and iron complexation behavior of lake sediment organic matter could provide valuable insights.

Our experiments indicate that the concentration of iron-complexing ligands in pig DOM is not high enough to significantly reduce iron and phosphorus precipitation from the solution. However, the morphology of precipitates formed in pig manure filtrate is substantially altered, suggesting that the influence of manure components on crystal formation may be both organic and inorganic. Further research into the specific organic and inorganic components in manure and their roles in crystallization processes would help clarify these interactions and optimize vivianite formation in complex matrices.

To mitigate the influence of organic ligands on vivianite formation, potential strategies should be explored. The carboxyl groups in compounds such as citrate and humate play a significant role in the binding of iron, increasing the affinity of these ligands for the metal. In matrices with high concentrations of such ligands, an effective approach could involve their separation prior to iron dosing using functionality-based resin adsorption. Alternatively, monitoring temporal changes in the iron-affinity of a given matrix – such as manure in this study - could help to identify optimal conditions for vivianite precipitation. This, in turn, would enhance the efficiency of the process.

5. Conclusion

This study investigated the influence of the iron-binding strength of organic ligands in manure compared to other organic ligands known to affect vivianite chemistry. By normalizing the impact of different organics on their DOC concentrations, ligands of varying complexity were

compared to their ability to dissolve or inhibit vivianite formation. Citrate strongly inhibited vivianite formation due to its high iron-binding affinity, while humate demonstrated the potential to kinetically outcompete vivianite formation. In contrast, pig DOM primarily affected the morphology and recoverability of precipitates but not due to the binding strength of the organics. These findings suggest that although iron-organic complexation can hinder vivianite formation, it is not always the primary mechanism behind reduced vivianite crystallization in complex matrices.

CRediT authorship contribution statement

Thomas Prot: Writing – review & editing, Supervision, Methodology, Conceptualization. **Julien Cottineau:** Writing – original draft, Investigation, Data curation. **Sophie Banke:** Writing – original draft, Methodology, Investigation, Formal analysis, Data curation, Conceptualization. **Mark C. M. van Loosdrecht:** Writing – review & editing, Supervision, Methodology, Conceptualization. **Leon Korving:** Writing – review & editing, Supervision, Methodology, Conceptualization.

Declaration of Generative AI and AI-Assisted Technologies in the Writing Process

During the preparation of this work the author(s) used Chat GPT in order to improve the writing style. After using this tool, the authors reviewed and edited the content as needed and take full responsibility for the content of the published article.

Declaration of Competing Interest

The authors declare that they have no known competing financial interests or personal relationships that could have appeared to influence the work reported in this paper.

Acknowledgment

This work was performed in the cooperation framework of Wetsus, European centre of Excellence for sustainable Water Technology (www.wetsus.eu). This work has received funding from the RecaP project within the European Union's Horizon 2020 Research and Innovation Program under grant agreement No 956454. Ruud Hendrikx at the Department of Materials Science and Engineering of the Delft University of Technology is acknowledged for the X-ray analysis. Thanks to all Wetsus theme members and RecaP partners for fruitful discussions.

Appendix A. Supporting information

Supplementary data associated with this article can be found in the online version at doi:10.1016/j.jece.2024.115139.

Data availability

Data will be made available on request.

References

[1] P. Wilfert, A.I. Dugulan, K. Goubitz, L. Korving, G.J. Witkamp, M.C.M. Van Loosdrecht, Vivianite as the main phosphate mineral in digested sewage sludge and its role for phosphate recovery, Water Res. 144 (2018), https://doi.org/10.1016/j.watres.2018.07.020.
[2] C. Li, Y. Sheng, H. Xu, Phosphorus recovery from sludge by pH enhanced anaerobic fermentation and vivianite crystallization, J. Environ. Chem. Eng. 9 (2021) 104663, https://doi.org/10.1016/j.jece.2020.104663.
[3] A. Al-Borno, M.B. Tomson, The temperature dependence of the solubility product constant of vivianite, Geochim. Cosmochim. Acta 58 (1994), https://doi.org/10.1016/0016-7037(94)90236-4.
[4] A. De Santiago, E. Carmona, J.M. Quintero, A. Delgado, Effectiveness of mixtures of vivianite and organic materials in preventing iron chlorosis in strawberry, Span. J. Agric. Res. 11 (2013) 208–216, https://doi.org/10.5424/sjar/2013111-2671.
[5] Y. Wu, J. Luo, Q. Zhang, M. Aleem, F. Fang, Z. Xue, J. Cao, Potentials and challenges of phosphorus recovery as vivianite from wastewater: a review, Chemosphere 226 (2019) 246–258, https://doi.org/10.1016/j.chemosphere.2019.03.138.
[6] W.K. Wijdeveld, T. Prot, G. Sudintas, P. Kuntke, L. Korving, M.C.M. van Loosdrecht, Pilot-scale magnetic recovery of vivianite from digested sewage sludge, Water Res. 212 (2022), https://doi.org/10.1016/j.watres.2022.118131.
[7] M. Rothe, A. Kleeberg, M. Hupfer, The occurrence, identification and environmental relevance of vivianite in waterlogged soils and aquatic sediments, Earth Sci. Rev. 158 (2016), https://doi.org/10.1016/j.earscirev.2016.04.008.
[8] T. Prot, 2021, Phosphorus recovery from iron-coagulated sewage sludge, Delft University of Technology, 2021, https://doi.org/10.4233/uuid:3d31068b-259a-4798-8723-be755cc15d23.
[9] L.K. ThomasArrigo, R. Kaegi, R. Kretzschmar, Ferrihydrite growth and transformation in the presence of ferrous iron and model organic ligands, Environ. Sci. Technol. 53 (2019), https://doi.org/10.1021/acs.est.9b03952.
[10] A. Abdelrady, S. Sharma, A. Sefelnasr, M. Kennedy, Characterisation of the impact of dissolved organic matter on iron, manganese, and arsenic mobilisation during bank filtration, J. Environ. Manag. 258 (2020), https://doi.org/10.1016/j.jenvman.2019.110003.
[11] S.E. Johnson, R.H. Loeppert, Role of organic acids in phosphate mobilization from iron oxide, Soil Sci. Soc. Am. J. 70 (2006), https://doi.org/10.2136/sssaj2005.0012.
[12] K. Lalonde, A. Mucci, A. Ouellet, Y. Gélinas, Preservation of organic matter in sediments promoted by iron, Nature 483 (2012), https://doi.org/10.1038/nature10855.
[13] A. Kleeberg, C. Herzog, M. Hupfer, Redox sensitivity of iron in phosphorus binding does not impede lake restoration, Water Res. 47 (2013), https://doi.org/10.1016/j.watres.2012.12.014.
[14] C. Simbeye, C. Courtney, P. Simha, N. Fischer, D.G. Randall, Human urine: a novel source of phosphorus for vivianite production, Sci. Total Environ. 892 (2023), https://doi.org/10.1016/j.scitotenv.2023.164517.
[15] P. Wilfert, P.S. Kumar, L. Korving, G.-J. Witkamp, M.C.M. van Loosdrecht, The relevance of phosphorus and iron chemistry to the recovery of phosphorus from wastewater: a review, Environ. Sci. Technol. 49 (2015), https://doi.org/10.1021/acs.est.5b00150.
[16] C. Zhang, D. Hu, R. Yang, Z. Liu, Effect of sodium alginate on phosphorus recovery by vivianite precipitation, J. Environ. Sci. 93 (2020), https://doi.org/10.1016/j.jes.2020.04.007.
[17] H. Cui, X. Yang, X. Gao, D. Sun, X. Cheng, Compatibility of vivianite-crystallization pathway of phosphorus recovery with anaerobic digestion systems of thermally hydrolyzed sludge, Environ. Res. 260 (2024) 119640, https://doi.org/10.1016/j.envres.2024.119640.
[18] X. Chen, M. Zheng, X. Cheng, C. Wang, K. Xu, Impact of impurities on vivianite crystallization for phosphate recovery from process water of hydrothermal carbonization of kitchen waste, Resour. Conserv. Recycl. 185 (2022) 106438, https://doi.org/10.1016/j.resconrec.2022.106438.
[19] C. Li, Y. Sheng, Organic matter affects phosphorus recovery during vivianite crystallization, Water Sci. Technol. 83 (2021), https://doi.org/10.2166/wst.2021.112.
[20] S. Yang, X. Yang, C. Zhang, S. Deng, X. Zhang, Y. Zhang, X. Cheng, Significantly enhanced P release from vivianite as a fertilizer in rhizospheric soil: effects of citrate, Environ. Res. 212 (2022), https://doi.org/10.1016/j.envres.2022.113567.
[21] S. Gypser, D. Freese, Phosphorus release from vivianite and hydroxyapatite by organic and inorganic compounds, Pedosphere 30 (2020), https://doi.org/10.1016/S1002-0160(20)60004-2.
[22] Q. Li, X. Liu, N. Hou, J. Wang, Y.-R. Wang, W.-Q. Li, J.-Q. Chen, Y. Mu, Roles of humic acid on vivianite crystallization in heterogeneous nucleation for phosphorus recovery, J. Clean. Prod. 367 (2022), https://doi.org/10.1016/j.jclepro.2022.133056.
[23] Y. Zhang, X. Yang, X. Zhang, D. Sun, X. Liu, R. Lan, M. Zheng, M.C.M. van Loosdrecht, X. Cheng, Proteins in hydrothermal carbonization liquor of sewage sludge interfere with vivianite crystallization for phosphorus recovery, Resour. Conserv. Recycl. 208 (2024) 107731, https://doi.org/10.1016/j.resconrec.2024.107731.
[24] E. Schütze, S. Gypser, D. Freese, Kinetics of phosphorus release from vivianite, hydroxyapatite, and bone char influenced by organic and inorganic compounds, Soil Syst. 4 (2020), https://doi.org/10.3390/soilsystems4010015.
[25] S. Gu, Y. Qian, Y. Jiao, Q. Li, G. Pinay, G. Gruau, An innovative approach for sequential extraction of phosphorus in sediments: ferrous iron P as an independent P fraction, Water Res. 103 (2016), https://doi.org/10.1016/j.watres.2016.07.058.
[26] Q. Wang, T.-H. Kim, K. Reitzel, N. Almind-Jørgensen, U.G. Nielsen, Quantitative determination of vivianite in sewage sludge by a phosphate extraction protocol validated by PXRD, SEM-EDS, and ^{31}P NMR spectroscopy towards efficient vivianite recovery, Water Res. 202 (2021), https://doi.org/10.1016/j.watres.2021.117411.
[27] K.D. Jacob, W.L. Hill, Fertilizer Technology and Resources in the United States, Academic Press, 1953.
[28] Z. Wang, W. Wang, P. Li, Y. Leng, J. Wu, Continuous production of volatile fatty acids (VFAs) from swine manure: determination of process conditions, VFAs composition distribution and fermentation broth availability analysis, Water 14 (2022), https://doi.org/10.3390/w14121935.
[29] W.S. Lee, A.S.M. Chua, H.K. Yeoh, G.C. Ngoh, A review of the production and applications of waste-derived volatile fatty acids, Chem. Eng. J. 235 (2014), https://doi.org/10.1016/j.cej.2013.09.002.

[30] J. Adusei-Gyamfi, B. Ouddane, L. Rietveld, J.-P. Cornard, J. Criquet, Natural organic matter-cations complexation and its impact on water treatment: a critical review, Water Res. 160 (2019), https://doi.org/10.1016/j.watres.2019.05.064.
[31] E.-H. Song, J. Shang, D.M. Ratner, Polysaccharides. Polymer Science: A Comprehensive Reference, Elsevier, 2012, https://doi.org/10.1016/B978-0-444-53349-4.00246-6.
[32] P.H. Struthers, D.H. Sieling, Effect of organic anions on phosphate precipitation by iron and aluminum as influenced by pH, Bull. Mass. Agric. Exp. Stn. 736 (1949) 205–213.
[33] J.M. Murphy, B.A. Powell, J.L. Brumaghim, Stability constants of bio-relevant, redox-active metals with amino acids: The challenges of weakly binding ligands, Coord. Chem. Rev. 412 (2020) 213253, https://doi.org/10.1016/j.ccr.2020.213253.
[34] P. Fejdi, J.-F. Poullen, M. Gasperin, Affinement de la structure de la vivianite Fe3 (PO4)2• 8 H2O, Bull. De. Min. éralogie 103 (1980), https://doi.org/10.3406/bulmi.1980.7386.
[35] R.R.U.F.F.T.M. Project, Rruff R040185. 2024.
[36] T. Šijakova - Ivanova, V. Zajkova-Paneva, L. Robeva - Čukovska, Mineralogical and chemical characterization of vivianite occurence in sediments of the pelagonia basin, rebublic of macedonia, Geol. Maced. 32 (2018).
[37] E.A. Karpukhina, D.S. Volkov, M.A. Proskurnin, Quantification of lignosulfonates and humic components in mixtures by ATR FTIR spectroscopy, Agronomy 13 (2023), https://doi.org/10.3390/agronomy13041141.
[38] D.C. Ashley, E. Jakubikova, Tuning the redox potentials and ligand field strength of Fe(II) polypyridines: the dual π-donor and π-acceptor character of bipyridine, Inorg. Chem. 57 (2018), https://doi.org/10.1021/acs.inorgchem.8b01002.
[39] E. Makrlík, P. Vañura, Stability constants of tris(2,2′-bipyridine) complexes of Fe2 + , Co2+ , Ni2+ , Cu2+ and Zn2+ in 1,2-dichloroethane saturated with water, Colloids Surf. 68 (1992), https://doi.org/10.1016/0166-6622(92)80204-F.
[40] D.R. BurgessNIST SRD 46. Critically selected stability constants of metal complexes: version 8.0 for windows, 2004, https://doi.org/10.18434/M32154.
[41] C. Catrouillet, M. Davranche, A. Dia, M. Bouhnik-Le Coz, R. Marsac, O. Pourret, G. Gruau, Geochemical modeling of Fe(II) binding to humic and fulvic acids, Chem. Geol. 372 (2014), https://doi.org/10.1016/j.chemgeo.2014.02.019.
[42] M. Yamamoto, A. Nishida, K. Otsuka, T. Komai, M. Fukushima, Evaluation of the binding of iron(II) to humic substances derived from a compost sample by a colorimetric method using ferrozine, Bioresour. Technol. 101 (2010), https://doi.org/10.1016/j.biortech.2010.01.050.
[43] F. Tambone, P. Genevini, G. D'Imporzano, F. Adani, Assessing amendment properties of digestate by studying the organic matter composition and the degree of biological stability during the anaerobic digestion of the organic fraction of MSW, Bioresour. Technol. 100 (2009), https://doi.org/10.1016/j.biortech.2009.02.012.
[44] B. Morgan, O. Lahav, The effect of pH on the kinetics of spontaneous Fe(II) oxidation by O2 in aqueous solution – basic principles and a simple heuristic description, Chemosphere 68 (2007) 2080–2084, https://doi.org/10.1016/j.chemosphere.2007.02.015.
[45] L. Wei, T. Hong, K. Cui, T. Chen, Y. Zhou, Y. Zhao, Y. Yin, J. Wang, Q. Zhang, Probing the effect of humic acid on the nucleation and growth kinetics of struvite by constant composition technique, Chem. Eng. J. 378 (2019), https://doi.org/10.1016/j.cej.2019.122130.
[46] L. Wei, T. Hong, H. Liu, T. Chen, The effect of sodium alginate on struvite crystallization in aqueous solution: a kinetics study, J. Cryst. Growth 473 (2017), https://doi.org/10.1016/j.jcrysgro.2017.03.039.
[47] M. Gould, E. Genetelli, Heavy metal complexation behavior in anaerobically digested sludges, Water Res. 12 (1978), https://doi.org/10.1016/0043-1354(78)90126-4.
[48] L.J. Kubeneck, L.K. ThomasArrigo, K.A. Rothwell, R. Kaegi, R. Kretzschmar, Competitive incorporation of Mn and Mg in vivianite at varying salinity and effects on crystal structure and morphology, Geochim. Cosmochim. Acta 346 (2023), https://doi.org/10.1016/j.gca.2023.01.029.
[49] C. Schott, J.R. Cunha, R.D. van der Weijden, C. Buisman, Phosphorus recovery from pig manure: Dissolution of struvite and formation of calcium phosphate granules during anaerobic digestion with calcium addition, Chem. Eng. J. 437 (2022) 135406, https://doi.org/10.1016/j.cej.2022.135406.
[50] S. Amjad, M.L. Christensen, K. Reitzel, H. Qu, Vivianite for phosphorus recovery from digester supernatant in wastewater treatment plants, Chem. Eng. Technol. 46 (2023), https://doi.org/10.1002/ceat.202300071.
[51] J.J. De Yoreo, Principles of crystal nucleation and growth, Rev. Miner. Geochem. 54 (2003), https://doi.org/10.2113/0540057.